Establishing Major Permeability Controls in the Mak-Ban Geothermal Field, Philippines

Ronald O. Vicedo[1], James A. Stimac[2], Vilma T. Capuno[1], and Jacob B. Lowenstern[3]

[1]Chevron Geothermal Philippines Holdings, Inc., Makati , Philippines
[2]Chevron Geothermal Salak, Jl. Asia-Afrika, Jakarta , Indonesia
[3]U.S. Geological Survey, Volcano Hazards Team, Menlo Park, CA, USA

Keywords

Mak-Ban, Bulalo, conceptual modeling, spherulitic rhyolite, volcanic facies, gamma ray, tracer test, $^{40}Ar/^{39}Ar$, U/Pb, naphthalene disulfonate

ABSTRACT

Recent updating of the conceptual model of the Mak-Ban (Bulalo) geothermal field verified both structural and stratigraphic controls on permeability and connectivity in the reservoir. Two silicic units within the predominantly andesitic production zone were identified from borehole logs, core and drill cuttings. Whole rock chemical data and petrographic analysis confirmed two rhyolite units that consist of partially welded ash-flow tuffs and lava with primary devitrification and vapor-phase alteration textures typical of subaerial rhyolites. U/Pb dating of zircons from the units showed two distinct episodes of silicic volcanism at 352 ± 16 ka and 501 ± 12 ka, respectively. A recent drilling campaign allowed the running of more gamma ray (GR) in tandem with PTS logs. The logs validated the presence of two units with high GR response generally coinciding with permeable zones just below the interpreted top of the reservoir.

Naphthalene disulfonate tracer testing defined a predominantly fault-controlled flow path of fluids from the edges of the field into the central production area. Fifteen to 25% of injected tracers were recovered in production wells over a five-year monitoring period. Peak arrival of tracer returns indicated average speeds between 0.1 to 1.3 m/hr, allowing for sufficient time for the fluids to heat up prior to re-emergence in production wells. Although faults are known to be important pathways in most geothermal reservoirs, the identification of specific structures with high connectivities in Mak-Ban provide an important insight on fluid migration from peripheral areas. This information is critical in preparing a reservoir management strategy for addressing the entry of cool marginal recharge into the center of the field.

Introduction

The Mak-Ban geothermal field, also known as Bulalo (Figure 1), is one of two fields being operated by Chevron Geothermal Philippines Holdings, Inc. (CGPHI) on behalf of the government-owned power generation company, the National Power Corporation (NPC). With a baseload capability of 402 MW, it represents 32% of the 1,272 MW total geothermal capacity developed by Chevron Geothermal and Power Operations (GPO) in the Philippines and Indonesia. Mak-Ban started commercial operations in 1979 making it one of the oldest operating geothermal fields in the country. The second CGPHI-operated field is the 234 MW Tiwi geothermal field which also started commercial operations in 1979. Together, the two fields supply roughly 10% of the total

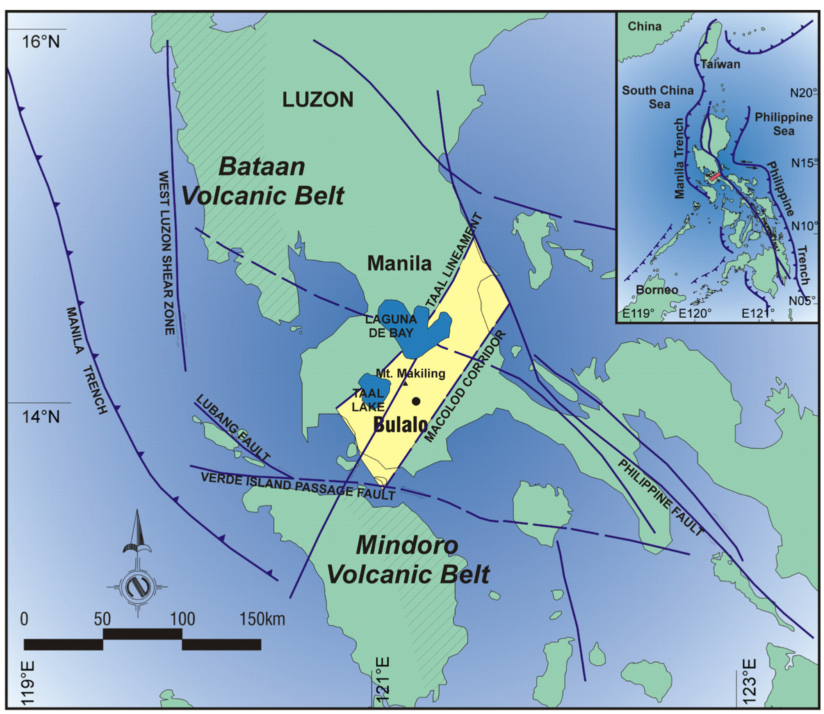

Figure 1. Macolod Corridor and Mak-Ban geothermal field geologic setting.

power demand of Luzon Island, meeting the electricity needs of about 3 million homes.

As geothermal fields mature, marginal fluids play an increasingly important role in well productivity and field performance. In the case of Bulalo, relatively cool marginal recharge has increasingly entered the reservoir as pressure has declined, contributing to reservoir cooling (Abrigo and Molling, 2003). Continuous and improved data collection and interpretation, and constant updating of the conceptual and numerical models are key factors that help ensure that such critical information is captured and fed into both short- and long-term resource management strategies. This paper summarizes studies on stratigraphy, structure, rock properties, and thermally-stable tracers that advanced our understanding of structural and stratigraphic controls on field permeability.

Geologic Setting

The Mak-Ban geothermal field lies within the central portion of the Macolod Corridor, a 40-kilometer wide NE-SW trending rift-like feature that perpendicularly crosses the NW-trending Luzon arc (Sudo et. al., 2000) (Figure 1). The structural setting of the Macolod Corridor is highly complex, being influenced by the active Philippine Fault and the more passive Verde Island Passage Fault, both major regional sinistral strike-slip faults. These two structures seem to enclose the corridor's NE and SW edges respectively, and impose on it a transtensional motion oriented NE-SW (Pubellier et. al., 2000). This NE-SW regional trend is further impressed on the Mak-Ban geothermal field in the form of major structures that influence fluid flow into the production sector (Figure 2).

Deformation in the NE-SW direction in the Macolod Corridor is also influenced by subduction of the Philippine Sea Plate in the east and Eurasian Plate/ Sundaland block in the west, which is responsible for the active volcanism, crustal thinning, extension and extensive normal and strike-slip faulting within the corridor (Galgana et. al., 2007). These tectonic processes resulted in the formation of young silicic calderas—e.g., Taal Volcano and Laguna Lake, andesitic to dacitic stratocone and dome complexes, and maar and cinder cone fields (Forster et. al., 1990).

Some studies have focused on explaining the origins of the abundant silicic rocks (with >65% SiO_2) in the Macolod Corridor. Interpretations vary from defining the source as subduction-related MORB-type mantle wedges that have undergone high degrees of partial melting with significant continental crust contamination (Defant et. al., 1991), to partial melting of calc-alkaline, mantle-derived, moderate to K-rich evolved magmas that have ponded and crystallized in the low to mid-crust (Vogel et. al., 2006) in the absence of any continental material. Silicic rocks play an important role in the Mak-Ban field, from being the source of the heat driving the geothermal system to providing pathways for fluid circulation across the field.

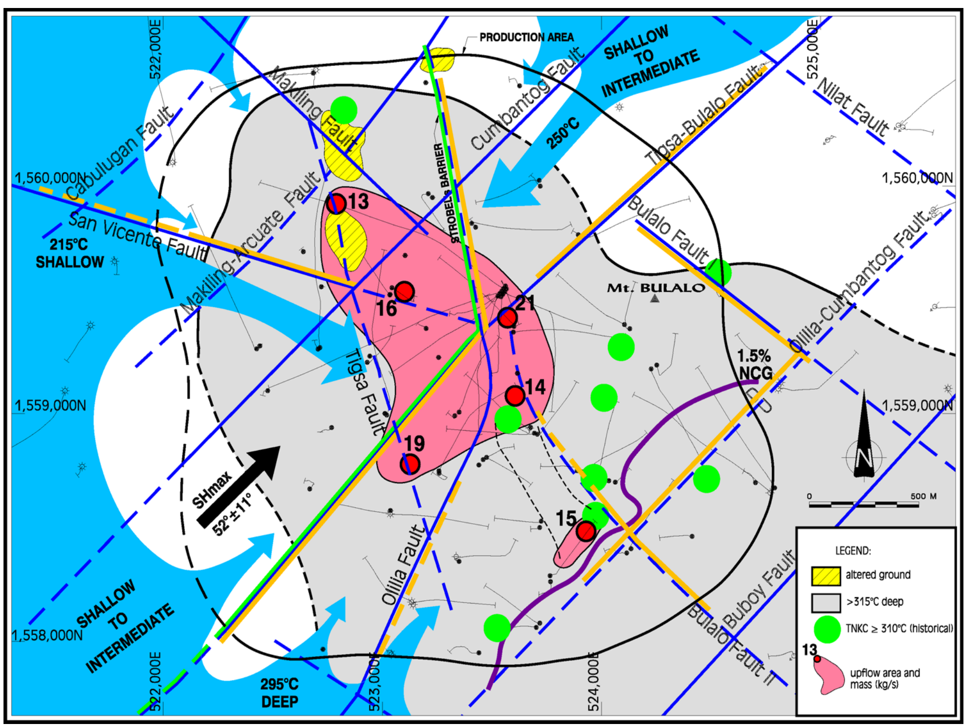

Figure 2. Key elements of the Mak-Ban conceptual model. Faults that act as semi-permeable barriers are highlighted in orange. Altered ground related to leakage from the system is shown in yellow. Areas of upflow are shown in magenta, along with the mass supplied in the numerical model in kg/s in black font. An area with deep measured temperatures ≥315°C is outlined in gray. This gray area encloses a smaller NW-trending region with measured temperatures >325°C and wells with historical NKC geothermometer temperatures >310°C. Areas of marginal recharge and its assumed temperature at the reservoir margin are outlined by the blue areas (arrows scaled to the amount). The high gas SE sector is delimited by the 1.5% NCG in steam contour in purple (adopted from Stimac et. al., 2006, unpublished report).

Conceptual Modeling

The conceptual model of Mak-Ban was created in 1999-2000 and updated in 2004-2005. The model highlighted the significance of particular structures acting either as flow conduits or barriers. The importance of certain lithologies in the reservoir with significant matrix and fracture permeability was also emphasized. A deep cooling magma body responsible for the emplacement of the Mt. Bulalo dacite dome is believed to be the heat source driving fluid circulation in the reservoir, through faults and permeable lithologic units.

The internal structure of Mak-Ban is largely dictated by faults. The confluence of several faults in the middle of the geothermal field coincides with the central upflow and "sweet spot", a zone defined by wells having high deliverability, stable decline rates, and constant wellbore chemistry suggesting vigorous basal recharge over time (Figure 2). Other faults act as pathways for injection returns and marginal recharge, defined by geochemistry as occurring in the NE, SW and NW, the original outflow directions prior to exploitation. Still others act as semi-permeable barriers as exemplified by the high NCG and high chloride brine portion in the southeast. The resource appears to be bounded in the NW by the Cabulugan fault while the Buboy fault is the possible SE boundary (Golla et. al., 2001). The model does not define NE and SW boundaries for the resource.

Although the importance of faults in the development and maintenance of fluid circulation in the reservoir was identified early on, quantifying the amount of produced injectate from particular injection wells and injection sectors has not been easy. Prior to 2001 it was difficult to conduct tracer tests in fields with temperatures >220°C because the available tracers (fluorescein and tinopal) were not thermally stable (Capuno et. al., 2007). New tracers (e.g. polyaromatic sulfonates such as naphthalene disulfonates or NDS) can now be used effectively at these temperatures to characterize the recoverability and speed of injection returns, and the connectivity between specific injection and production wells.

Volcanic Facies Modeling

Prior to the 10-well drilling campaign in 2002-2005, a review of the lithologies and stratigraphy in six representative wells near the central production area (Bul-97, Bul-99, Bul-100, Bul-101, Bul-102 and Bul-103) was conducted. Gamma ray (GR) and Schlumberger Formation Micro Scanner^{TM} (FMS) logs from these wells enabled good correlations between lithologic units to be made there (Stimac et. al., 2002; Dimabuyu et. al., 2005). Correlations there are limited to the interval between 450 m-bsl and 1,830 m-bsl; data below 1,830 m-bsl is limited. In this first stage of the review, it became clear that there were two units just below the top of the reservoir that had higher GR responses compared to the predominant andesitic and minor basaltic units that showed flatter GR responses (Table 1). A comparison with the location of permeable entry zones also indicated these were ideal zones for production.

Table 1. Summary of gamma ray (GR) values in API units and SiO_2 contents for different rock compositions in wt%. GR is the gamma ray value observed. SiO_2 content is based on IUGS classification. K, U, and Th concentrations are based on whole-rock chemistry from XRAL (unpublished report). Note that the GR values may vary from well to well, depending on wellbore conditions during logging, so this approach is qualitative (Dimabuyu et. al., 2005).

Lithology	GR (API)	SiO_2 (%)	K (%)	U (ppm)	Th (ppm)
Basalt	0-20	45-52	0.12 - 1.12	2.4 – 2.6	0.7 – 1.8
Andesite	20-30 (basaltic andesite) 30-90 (andesite)	52-57 57-63	0.17 – 4.25	2.1 – 16.0	0.6 – 4.4
Dacite	90 - >100	63-68	2.29 – 3.93	12.2 – 13.0	1.8 – 4.8
Rhyolite	***>100***	***>68***	***3.06 - 6.09***	***11.7 – 18.7***	***1.9 – 8.2***

In addition to the six wells, lithologic correlations were extended to wells from which thin sections had been made. Petrographic descriptions by several authors, most notably the latest study by Stimac (2001, unpublished internal report), were used to project lithologies beyond the area covered by the six wells. The sampling frequency of 200 ft was useful in identifying thick and distinctive units, but could not provide good resolution for thin or discontinuous units, nor give an accurate depth for the top or bottom of a rock unit. Nonetheless, the petrographic studies did confirm the presence of rhyolites as partially welded ash-flow tuffs and lava with unique primary devitrification and vapor-phase alteration textures typical of subaerial rhyolitic volcanics.

Other data used were whole-rock chemistry (Table 1), and porosity and permeability (Table 2). Whole-rock chemistry data were obtained on 24 core samples. Porosity and permeability data, included analysis done by TerraTek in 2002 and Core Labs data in 1997, correlated with the petrographic summary by Stimac in 2001 (all unpublished reports).

A facies model, developed using silicic caldera systems as analogs, suggested that the major silicic units were most likely outflow sheets, interbedded locally with lava domes and reworked epiclastic deposits. Key features that lead to enhanced permeability in such outflow sheets include their continuous lateral extent, extensive vertical jointing within some cooling units, and vapor-phase crystallization that tends to preserve a significant pore volume while strengthening the rock and rendering it relatively impervious to subsequent hydrothermal alteration. Given the wide range of potential thicknesses and depositional and cooling histories of outflow sheets, not all such deposits will have enhanced permeability. However, other examples of permeable outflow sheets have been observed, such as those in the Awibengkok geothermal field (Stimac et. al., in press). Caldera-filling ash-flow tuffs do not typically exhibit the same characteristics. Rapid burial in a rift setting also tends to minimize destruction of pore space that is typical in older volcanic sequences.

To constrain the age of the volcanic section and shed light on the volcano-tectonic evolution of the area, $^{40}Ar/^{39}Ar$ and U-Pb ages were obtained on selected surface and subsurface samples. $^{40}Ar/^{39}Ar$ dates on hornblende from the Bulalo and Olila dacite domes indicate that volcanism in the Mt. Makiling area occurred at <20,000 yrs B.P. U-Pb ages on individual zircons were obtained with the USGS-Stanford SHRIMP RG to constrain the age of two spherulitic rhyolite units SR1 and SR2 identified in the facies model. The ages verified that these two units represent two distinct episodes of silicic volcanism. SR1 from Bul-14, taken from 3,420 ft-MD (1,042 m), yielded a mean age of 352,000 ± 16,000 yrs. Zircons from Bul-56, -93 and -90, all from SR2 sampled from 3,469-7,604 ft-MD (1,057-2,319 m) had mean ages of 497,000 ± 13,000, 499,000 ± 11,000, and 506,000 ± 11,000 yrs, respectively. These ages highlight the very rapid accumulation of volcanic-sedimentary sequences in the extending Macolod Corridor.

Wells drilled during the ten-well drilling campaign completed in 2005 had an average of 3,110 m-MD

Table 2. Summary of porosity and permeability values for various lithologic types in the Bulalo reservoir (after TerraTek, 2002 and Core Labs, 1997).

Lithologic Type	Porosity, ϕ (%)		Permeability, K_{air} (mD)	
	Range	Average	Range	Average
Basalt lava	0.6 – 12.6	7.8	<0.01 – 1.3	0.4
Andesite lava	0.2 – 22.8	7.5	<0.01 – 6.3	1.19
Andesite ash-flow tuff	3.1 – 29.4	20.0	0.7 – 0.8	0.79
Andesite epiclastic & tuff	20.4 – 22.8	21.9		
Andesite fallout tuff	13.8 – 16.82	15.37	0.04 – 0.12	0.08
Dacite lava	3.7 – 11.3	8.1	1.6	1.6
Dacite ash-flow tuff	18.4 – 22.0	20.2	0.45 – 2.2	1.33
Dacite fallout	6.9	6.9	0.17	0.17
Dacite lahar	12.4 – 21.8	17.1		
Rhyolite lava	***7.8 – 20.4***	***15.5***	***0.66 - 0.83***	***0.75***
Intrusion	2.5	2.5	<0.01	<0.01

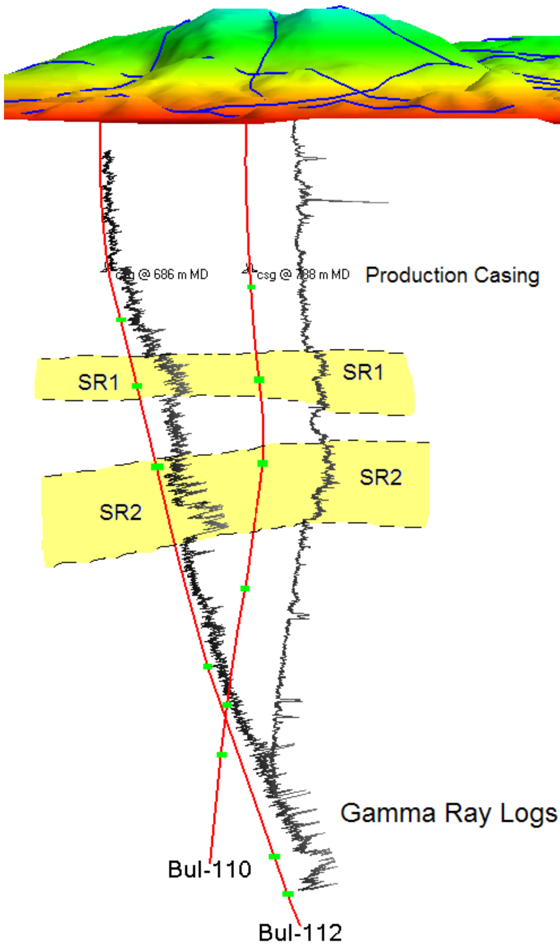

Figure 3. Gamma Ray log profiles in Bul-110 and -112 showing permeable zones (green markers), and the locations of SR1 and SR2.

(2,985 m vertical depth; VD). These were drilled much deeper than the previous 103 wells, which averaged only 2,150 m-MD (2,110 m-VD). GR logs were run in all ten wells upon completion. PTS (pressure, temperature and spinner) logs confirm the presence of fluid entries in the two spherulitic rhyolite units characterized by high gamma ray responses (Figure 3). Entry zones within the units would vary from well to well but in general, entry zones that could be correlated with the units occurred either near the upper or lower contacts, or within the central portion of the units.

Tracer Testing

Recent tracer testing helped refine the structural flow paths from injection wells on the edges of the field. Naphthalene disulfonate tracers were injected into wells ranging from 0.7 to 2.4 km from the nearest production well (Figure 4). In the eastern hot brine injection sector, 1-ns was injected into Bul-50 and 1,6-nds was injected into Bul-78. In the west, 2-ns, 2,6-nds and 2,7-nds were injected into hot brine injectors Bul-73, Bul-58 and Bul-75, respectively. 1,5-nds was injected into condensate injector Bul-69. Multiple tracers were found in wells in the center of the Bulalo field where several structures converge.

The tracer return patterns generally indicated preferential flow oriented NE-SW. This is best exemplified by 1,5-nds injected in Bul-69 which shows a direct connection with the central wells via the NE-SW trending Tigsa-Bulalo Fault. For the most part, long peak recovery times of tracers hinted sufficient heating of injected fluids could occur before reaching the production area. Calculated return rates ranged from 0.1 to 1.3 m/hr for all tracers, with tracer recoveries ranging from a high of 25% (for 1,5-nds injected in Bul-69 that exhibited the most direct path between injector and producers) to a low of 15% (for 2,6-nds injected in Bul-58). The return rates were calculated from five years of continuous sampling and monitoring (Capuno et. al., 2007). Some compartmentalization was observed as well, with the tracers injected in Bul-73 in the NW having zero recovery in all production wells monitored.

In addition, it was established that the connectivity between the production and injection wells is not controlled solely by the distance separating them. Bul-69, -04 and -11 are all located along the western side of the NE-SW trending Tigsa-Bulalo Fault (Figure 4). Bul-04 (drilled to a depth of 2,502 m-MD) is only 1.6 km from Bul-69. However, tracers were produced in Bul-04 one hundred days later than in Bul-11 (drilled to 1,062 m-MD) which is located 3.6 km from the injection well. The explanation for this occurrence was found in the lithology intersected by Bul-11, in particular the permeable spherulitic rhyolite unit in the shallow reservoir which it shares with the Bul-69 injector. Bul-04 does not have an entry zone at this shallow depth.

Figure 4. Fluid flowpaths inferred from naphthalene disulfonate tracer tests. Arrows show inferred tracer flow path from recovery patterns. Numbers on arrows mark the time of first/peak arrival of the tracer in days.

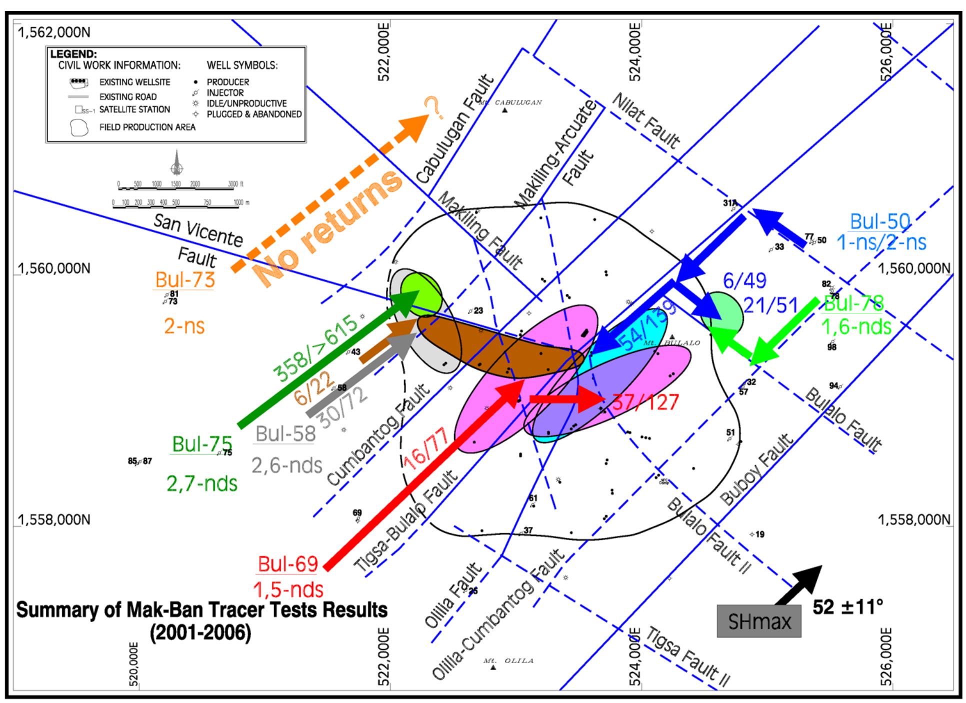

Conclusions

Recent studies confirm that particular structures and lithologies exert significant control over permeability and connectivity in the Mak-Ban geothermal field.

Two distinctive rhyolitic units (SR1 and SR2) occur just below the interpreted top of the reservoir and generally coincide with shallow production zones.

Naphthalene disulfonate tracer testing showed preferential flow of injected fluids in the NE-SW direction, consistent with the structural grain of the Macolod Corridor. This direction parallels the direction of maximum horizontal stress established through geomechanical studies.

Estimated speeds of 0.1 to 1.3 m/hr, peak arrival times after one year monitoring, as well as 15-25% recovery of tracers over a five-year monitoring period, all indicate little thermal breakthrough can be expected from brine and condensate injected in the edges of the field.

This information on major permeability controls will be useful in addressing the long term sustainability of the field by implementing strategies to mitigate the entry of cooler marginal fluids that have recently been identified encroaching into the main production area.

References

Abrigo, F.V., P.A. Molling, and J.A. Acuña, 2004. "Determination of Recharge and Cooling Rates Using Geochemical Constraints at the Mak-Ban (Bulalo) Geothermal Reservoir, Philippines." Geothermics 33, p. 11-36.

Capuno, V.T. and L.B. Villasenor, 2007. "Tracer Tests in the Tiwi and Mak-Ban Fields." Proceedings of the 28th Annual PNOC EDC Geothermal Conference, p. 153-159.

Clemente, W.C. and F.L. Villadolid-Abrigo, 1993. "The Bulalo Geothermal Field, Philippines: Reservoir Characteristics and Response to Production." Geothermics, v. 22 (5/6), p. 381-394.

Defant, M.J., R.C. Maury, E.M. Ripley, M.D. Feigenson, and D. Jacques, 1991. "An Example of Island-Arc Petrogenesis: Geochemistry and Petrology of the Southern Luzon Arc, Philippines." Journal of Petrology, Volume 32, Part 3, p. 455-500.

Dimabuyu, A.C., J.A. Stimac, D.P. Aquino, and J.B. Lowenstern, 2005. "An Age-calibrated Volcanic Facies Model of the Bulalo Geothermal Field, Philippines." AGU Chapman Conference on the Effects of Basement, Structure, and Stratigraphic Heritages on Volcano Behavior, Program and Abstracts Volume p. 12.

Forster, H., D. Oles, U. Knittel, M.J. Defant, and R.C. Torrres, 1990. "The Macolod Corridor: a Rift Crossing the Philippine Island Arc." Tectonophysics 183, p. 265-271.

Galgana, G., M. Hamburger, R. McCaffrey, E. Corpuz, and Q. Chen, 2007. " Analysis of Crustal Deformation in Luzon, Philippines Using Geodetic Observations and EarthQuake Focal Mechanisms." Tectonophysics 432, p. 63-87.

Golla, G. U., F.V. Abrigo, B.O. Alarcon, P.A. Molling, and J.A. Stimac, 2001. "The Bulalo Geothermal Field, Philippines: Conceptual Model of a Prolific Geothermal System." Proceedings of the 22nd Annual PNOC-EDC Geothermal Conference, p. 123-132.

Pubellier, M., F. Garcia, A. Loevenbruck, and J. Chorowicz, 2000. "Recent Deformation at the Junction Between the North Luzon Block and the Central Philippines from ERS-1 Images." Island Arc 9 (4), p. 598–610.

Stimac, J.A., F.V. Abrigo, J. Acuna, B.A. Arcedera, G.J. Batayola, V.T. Capuno. A.C. Dimabuyu, A.J. Menzies, J.A.P. Protacio, and R.O. Vicedo, 2005. "2005 Bulalo Conceptual and Numerical Model Update." Unpublished Internal Technical Report, Unocal Philippines, Inc.

Stimac, J.A., A.C. Dimabuyu, and F.J. Sugiaman, 2002. "Detailed Stratigraphy and Facies Model of the Bulalo Geothermal Field." Presented at the 15th Annual Geological Society of the Philippines Geological Convention, Philippines, December 2002.

Stimac, J.A., G.A. Nordquist, A. Suminar, and L. Sirad-Azwar, 2008. "An overview of the Awibengkok Geothermal System, Indonesia." Geothermics, in press.

Sudo, M., E.L. Listanco, N. Ishikawa, T. Tagami, H. Kamata, and Y. Tatsumi, 2000. "K-Ar Dating of the Volcanic Rocks from the Macolod Corridor in Southwestern Luzon, Philippines: Toward Understanding of the Quaternary Volcanism and Tectonics." AGU 2000 Western Pacific Geophysics Meeting V22A-05.

Vogel, T.A., T.P. Flood, L.C. Patino, M.S. Wilmot, R.P.R. Maximo, C.B. Arpa, C.A. Arcilla, and J.A. Stimac, 2006. "Geochemistry of Silicic Magmas in the Macolod Corridor, SW Luzon, Philippines: Evidence of Distinct, Mantle-Derived, Crustal Sources for Silicic Magmas." Contributions to Mineralogy and Petrology 151 (3), p. 267-281.